

# Surface Monitoring of Surfactant Phase Separation and Stability in Waterborne Acrylic Coatings

Dominique Scalrone,<sup>\*,†</sup> Massimo Lazzari,<sup>†,‡</sup> Valter Castelvetro,<sup>‡,§</sup> and Oscar Chiantore<sup>†</sup>

*NIS Centre of Excellence and Dipartimento di Chimica IFM, University of Torino, Via P. Giuria 7, 10125 Torino, Italy; Dipartimento di Chimica e Chimica Industriale, University of Pisa, Via Risorgimento 35, 56126 Pisa, Italy; and PolyLab-CNR, via Risorgimento 35, 56126, Pisa, Italy*

*Received May 24, 2007. Revised Manuscript Received August 28, 2007*

The stability of a waterborne acrylic coating has been studied paying particular attention to the effects of surfactants (SDS and Triton X-405). In a latex, surfactants are a minor component with respect to the polymer matrix, but they are of fundamental importance in stabilizing the polymer particles in the aqueous medium. When the coating has dried, they exude to the interfaces and self-assemble into hydrophilic aggregates that protrude from the film surface. The surfactant surface distribution has been monitored during thermal and light aging, and the changes observed have been investigated both in terms of the diffusion behavior of low molecular weight molecules in a polymer matrix and in terms of the chemical stability of the surfactants themselves.

## Introduction

Waterborne coatings are obtained from polymer particles dispersed in an aqueous medium and stabilized by surfactants. Since their introduction in the market, waterborne vinyl and acrylic coatings have been used in a number of applications; among them it is worth mentioning wall paints, protective coatings, liquid and heat-set adhesives, and consolidants for stone, paper, and textile.

More recently the introduction of new environmental legislation aimed at drastically reducing the use of volatile organic compounds has promoted the research activity on solvent-free methodologies and products. Besides environmental aspects, waterborne polymers are also appreciated for the flexibility of formulations, the large reduction in viscosity, compared to polymer solutions, and a more efficient heat transfer during the polymerization process.

In the past few years, some of the present authors have investigated a wide range of films obtained from commercial acrylic latexes and paints as well as laboratory-made products. The earlier studies were aimed at the identification of the components of waterborne coatings and emulsion paints (polymer fraction, surfactants, protective colloids, thickeners, stabilizers, pigments, antifoam agents, biocides,

etc.);<sup>1,2</sup> later on, acrylic coating samples aged under natural indoor and accelerated laboratory conditions were investigated.<sup>3</sup>

The present work is mainly focused on surface morphological and chemical changes that have occurred on thin acrylic coatings during film formation and subsequent aging treatments.

The transformation from a colloidal aqueous dispersion to a continuous polymer layer occurs through several steps involving water evaporation, packing of polymer particles, their deformation, and coalescence (i.e., interparticle diffusion of polymer molecules resulting in an isotropic coating).<sup>4–6</sup> A number of theories and models have been proposed to describe film formation and particle deformation, and each of them takes into account, although with different emphasis, the relative weight of different forces such as the various van der Waals, capillary, gravitational, electrostatic, elastic, surface, and interface forces.<sup>7–10</sup> Despite the continuing discussion on the forces and mechanisms involved in the formation of a film from a polymer dispersion, it is clear that this process is favored when the forces that oppose particle deformation are minimized, and this is essentially obtained by lowering the glass transition temperature ( $T_g$ ).<sup>11</sup>

However, a number of papers have pointed out that the evolution of the film properties can be strongly affected not only by the  $T_g$  and the polymer composition but also by the surfactants. In particular, in addition to their essential function

\* Corresponding author: phone +39 011 6707546; Fax +39 011 6707855; e-mail dominique.scalarone@unito.it.

<sup>†</sup> University of Torino.

<sup>‡</sup> University of Pisa.

<sup>§</sup> PolyLab-CNR.

<sup>‡</sup> Present address: Department of Physical Chemistry, Faculty of Chemistry, University of Santiago de Compostela, 15782 Santiago (La Coruña), Spain.

(1) Chiantore, O.; Scalrone, D.; Learner, T. J. S. *Int. J. Polym. Anal. Charact.* **2003**, *8*, 67.

(2) Scalrone, D.; Chiantore, O. *J. Sep. Sci.* **2004**, *27*, 263.

(3) Scalrone, D.; Chiantore, O.; Learner, T. *Ageing studies of acrylic emulsion paints. Part II. Comparing formulations with poly(EA-co-MMA) and poly(nBA-co-MMA) binders*; Preprints ICOM Committee for Conservation 13th Triennial Meeting, Rio de Janeiro; James & James (Science Publishers): London, UK, 2002; pp 911–919.

(4) Feng, J.; Winnik, M. A. *Macromolecules* **1997**, *30*, 4324.

(5) Vanderhoff, J. W. *Br. Polym. J.* **1970**, *2*, 161.

(6) Wang, Y.; Kats, A.; Juhùè, D.; Winnik, M. A. *Langmuir* **1992**, *8*, 1435.

(7) Lin, F.; Meier, D. J. *Prog. Org. Coat.* **1996**, *29*, 139.

(8) Dillon, R. E.; Matheson, L. A.; Bradford, E. B. *J. Colloid Sci.* **1951**, *6*, 108.

(9) Brown, G. L. *J. Polym. Sci.* **1956**, *22*, 423.

(10) Sheetz, D. P. *J. Appl. Polym. Sci.* **1965**, *9*, 3759.

(11) Keddie, J. L.; Meredith, P.; Jones, R. A. L.; Donald, A. M. *Macromolecules* **1995**, *28*, 2673.

of providing the nucleation sites for the growth of polymer particles during the free radical reaction and of stabilizing the polymer particles in the aqueous medium after the polymerization, surfactants can also interfere in the film formation. In fact, as water evaporates and the polymer particles become closer, the adsorbed surfactants may negatively affect particle coalescence. As a result, surfactants can significantly alter the final performances and properties of the coating and especially the interfacial properties such as wettability and adhesion. Urban et al. demonstrated that anionic surfactants such as sodium dodecyl sulfate (SDS) and sodium dioctylsulfosuccinate (SDOSS) migrate to the film–air interface and take preferential orientations; the surfactant hydrophobic tails are preferentially perpendicularly oriented, while the hydrophilic groups exhibit preferential parallel orientation.<sup>12,13</sup> The distribution of surfactants throughout the depth of the film is mainly due to the water evaporation rate: if the latter is fast and surfactants are allowed to follow the water front, then they concentrate in the upper part of the film; if the evaporation rate is low, the surfactant distribution is more homogeneous.<sup>14</sup> After water loss, diffusion becomes the only possible mechanism of transport for low molecular weight species. Surfactant diffusion depends on their solubility in the polymer matrix and on the tendency of the polymer particles to coalesce.<sup>15,16</sup> When the surfactants are chemically compatible with the polymer, they dissolve and plasticize the film; otherwise, they exude to the film–air and film–substrate interfaces or self-segregate within the film to form inverted micelles or even larger hydrophilic domains that increase the heterogeneity of the coating.<sup>17</sup> Overall, coalescence promotes surfactant desorption from the polymer particles and migration to the film–air and film–substrate interfaces.

Although the film formation process of waterborne coatings and the distribution of water-soluble and surface-active species in latex films have already been debated in the scientific literature, there are still several aspects open for discussion. This study focuses on one of those aspects, the fate of surfactants, not only in terms of distribution in the solid film but also considering their intrinsic lifetime. This last point has been underestimated until now, but the effects that surfactants have on bulk and surface properties of waterborne coatings certainly depend on their physical form and chemical stability.

## Experimental Section

**Synthesis of the Acrylic Latex.** The acrylic latex was synthesized by seeded starved-feed semicontinuous copolymerization of a 70/30 w/w mixture of methyl methacrylate (MMA) and butyl acrylate (BA). The seed latex was prepared by batch emulsion polymerization (15 min at 80 °C) of the comonomers' mixture (0.72

g in 12 mL of unbuffered deionized water) in the presence of ammonium persulfate (50 mg) and a mixture of anionic (sodium dodecyl sulfate, SDS) and nonionic (Triton-X405, Fluka, a polyethoxylated octylphenol with 40 oxyethylene units) surfactants (60 mg each) to give a 6% total solids dispersion. To the seed latex stirred at 80 °C and 250 rpm in a 250 mL jacketed glass reactor was slowly added with a metered syringe pump an emulsion with the same comonomers composition as the seed (9.3 g in 45 mL of water containing 0.4 g of SDS); the polymerization was completed with a further 2 h stirring at 80 °C. Starved feed conditions were adopted to ensure uniform copolymer composition. The resulting latex had a 15 wt % solids content, 4.6 phr (parts per hundreds of resin, by weight) of SDS, and 0.6 phr of Triton X-405. The latex polymer particles had an average diameter of 59 nm, as measured by dynamic light scattering with a Brookhaven 90 Plus instrument.

**Latex Films.** The acrylic films were prepared by casting the latex on glass slides or silicon wafers and drying for 3 days at ambient conditions before analysis and aging treatments.

**Aging Procedure.** Once dried, the acrylic films were aged under different conditions: thermal aging at 60 and 120 °C and light aging. Isothermal aging was carried out in a forced air circulation oven. To simulate outdoor solar exposure, a Suntest CPS apparatus (Heraeus, Germany) was used, equipped with a xenon lamp and a UV filter that absorbs wavelengths lower than 295 nm. The irradiation power was set at 765 W/m<sup>2</sup>, and during the aging the maximum temperature recorded on the samples was 45 °C.

**Fourier Transform Infrared Spectroscopy (FTIR).** For the infrared analysis in the transmission mode, films with thickness in the range of 10–20 μm were cast on silicon wafers. Spectra were collected with a Thermo-Nicolet FT-IR Nexus instrument with a DTGS detector and a 4 cm<sup>-1</sup> resolution.

Attenuated total reflectance (ATR) spectra of films prepared on glass slides were collected with a Thermo Nicolet Smart Endurance device.

For micro-ATR mapping, a Thermo-Nicolet Continuum infrared microscope was used. The instrument is equipped with a silicon crystal ATR objective, which allows nondestructive microscopic surface analysis, and with a motorized stage to provide fully automated mapping. Maps of 700 × 700 μm were analyzed, with a space resolution of 70 μm.

**Atomic Force Microscopy (AFM).** AFM analyses were performed in air at room temperature with a Park Scientific Instruments AutoProbe LS and silicon cantilevers equipped with conical silicon tips. Images were collected in both contact and tapping mode.

## Results and Discussion

Thin films were prepared from a butyl acrylate/methyl methacrylate 30/70 copolymer latex synthesized by seeded semicontinuous emulsion polymerization. The feed composition was aimed at a copolymer with a glass transition slightly above room temperature ( $T_g = 35$  °C) to better discriminate and possibly emphasize the effects of thermal annealing on the bulk and surface properties of the latex film. A relatively large amount of surfactants was used in the first stage of the seeded polymerization (a 1/1 mixture of an anionic and a nonionic surfactant, about 8 phr, parts per hundred of resin, each) to facilitate the subsequent investigation on the surfactant migration during and after film formation. Most of the anionic surfactant SDS and all of the nonionic Triton X-405 used as colloidal stabilizers were introduced in this first stage, resulting in a final latex composed of small polymer particles (average diameter was 59 nm) with a

(12) Niu, B.-J.; Urban, M. W. *J. Appl. Polym. Sci.* **1996**, *60*, 371.

(13) Zhao, Y.; Urban, M. W. *Langmuir* **2001**, *17*, 6961.

(14) Mallécol, J.; Gorce, J.-P.; Dupont, O.; Jeynes, C.; McDonald, P. J.; Keddie, J. L. *Langmuir* **2002**, *18*, 4478.

(15) Belaroui, F.; Hirn, M. P.; Grohens, Y.; Marie, P.; Holl, Y. *J. Colloid Interface Sci.* **2003**, *261*, 336.

(16) Song, M.; Hourston, D. J.; Pang, Y. *Prog. Org. Coat.* **2000**, *40*, 167.

(17) Aramendia, E.; Mallécol, J.; Jeynes, C.; Barandiaran, M. J.; Keddie, J. L.; Asua, J. M. *Langmuir* **2003**, *19*, 3212.

**Table 1. FTIR Characteristic Vibration Modes of Poly(nBA-co-MMA)**

wavenumber (cm <sup>-1</sup> )	vibration mode
2956	$\nu_a(\text{C-H})$ CH <sub>3</sub>
2930	$\nu_a(\text{C-H})$ CH <sub>2</sub>
2874	$\nu_s(\text{C-H})$ CH <sub>2</sub>
2847	$\nu_s(\text{C-H})$ skeleton CH <sub>2</sub>
1726	$\nu(\text{C=O})$
1447	$\delta(\text{CH}_2)$ CH <sub>2</sub>
1385	$\delta(\text{CH}_2)$ CH <sub>3</sub>
1238	$\nu(\text{C-O})$ COC
1141	$\nu(\text{C-O})$ COC
1066	$\nu(\text{C-O})$ OOC
990	$\rho\text{CH}_3$ (MMA)
960	$\rho\text{CH}_3$ (nBA)
840	vibration of the side chain (nBA)
752	vibration of the side chain (MMA)

relatively narrow size distribution; uniform copolymer composition was ensured by the starved feed procedure adopted in the final semicontinuous stage.

The as-cast latex films were dried several days at room temperature, followed by thermal or light aging; the ensuing chemical changes were monitored by infrared spectroscopy. Atomic force microscopy was used to analyze the changes in surface morphology due to either chemical (i.e., thermal and photooxidative degradation) and physical (i.e., film formation, exudation of low molecular weight compounds) aging phenomena.

**Thermal and Photooxidative Stability of Waterborne Acrylic Coatings Monitored by Infrared Spectroscopy.** The thermal and photostability of acrylic polymers is generally very high, but under accelerated aging conditions both cross-linking reactions involving the polymer backbone and scissions on the side ester groups develop, resulting in the loss of volatile molecules and the formation of hydroxyl groups and new carbonyl functionalities.<sup>18–20</sup> Thermal aging, even after a thousand hours of treatment, showed no significant spectral changes. On the contrary, solar light irradiation induced photooxidative degradation reactions, as shown by the increased hydroxyl absorption at 3250 cm<sup>-1</sup> and the broadened carbonyl peak at 1730 cm<sup>-1</sup>. The other main vibration modes of the acrylic copolymer are listed in Table 1.

In order to differentiate between bulk and surface effects from the aging treatments, the films were comparatively analyzed by infrared spectroscopy in transmission mode and by attenuated total reflectance (ATR)-FTIR.

The ATR-FTIR spectra of thermally aged acrylic films showed additional features (Figure 1): an absorption centered at 1420 cm<sup>-1</sup> that overlaps with the peaks due to the bending vibrations of the methylene and methyl groups and a relatively intense absorption at 1100 cm<sup>-1</sup>, which appears as a shoulder of the  $\nu(\text{C-O})$  stretching of the acrylic copolymer. These two bands, which were not detected in transmission mode, were likely related to the enrichment of the film surface in one or more of the latex components. In particular, it was suspected that the above features could be

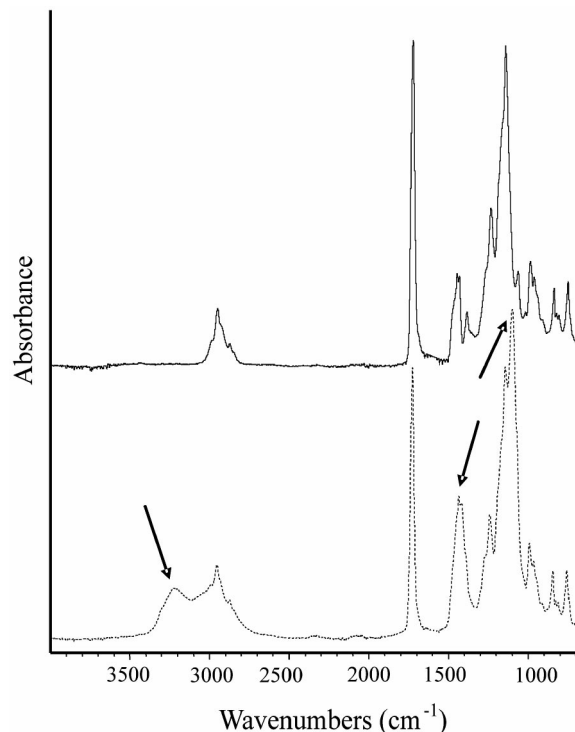


**Figure 1.** ATR-FTIR spectra of the acrylic latex film soon after drying (solid line) and after 500 h of accelerated photoaging (dashed line). Arrows indicate the main spectral changes occurring during aging.

due to the buildup of SDS aggregates at the polymer–air interface as a result of the migration of this low molecular weight surfactant from the bulk to the top of the film. This hypothesis was confirmed by the disappearance of the two additional peaks after rinsing of the sample surface with distilled water. However, the additional peaks do not match with the infrared spectrum of SDS, presenting its most intense absorption peaks at different wavenumbers (Figure 2a): the asymmetric and symmetric methylene stretching at 2918 and 2850 cm<sup>-1</sup>, the asymmetric methyl stretching at 2955 cm<sup>-1</sup>, the (CH<sub>2</sub>)<sub>n</sub> deformation vibration at 1468 cm<sup>-1</sup>, the strong doublet at 1250–1220 cm<sup>-1</sup> due to asymmetric  $-(\text{SO}_2)-$  stretching, the symmetric  $-(\text{SO}_2)-$  stretching at 1078 cm<sup>-1</sup>, and the sulfate bending vibration at 590 cm<sup>-1</sup>.<sup>21</sup> In fact, the substance detected on the surface of the thermally aged latexes by ATR is degraded SDS. In the next paragraph the spectral changes occurring to sodium dodecyl sulfate and polyethoxylated surfactants during accelerated aging will be discussed.

**Thermal and Photooxidative Stability of SDS and Triton X Surfactants.** As a further step, it was decided to investigate the stability of SDS as well as Triton X-405, another common surfactant used in the formulation of the latex, and to monitor their spectral changes during light and thermal aging. SDS is stable during artificial solar light irradiation, but at 120 °C it degrades relatively quickly. Figure 2 shows the FTIR spectra of SDS after 48 and 500 h of thermal aging. Among the most important changes there were the appearance of the same absorptions detected on the surface of the aged acrylic latex film: a broad  $\nu(\text{O-H})$

(18) Lazzari, M.; Chiantore, O. *Polymer* **2000**, *41*, 6447.

(19) Chiantore, O.; Lazzari, M. *Polymer* **2001**, *42*, 17.

(20) Chiantore, O.; Trossarelli, L.; Lazzari, M. *Polymer* **2000**, *41*, 1657.

(21) Socrates, G. *Infrared and Raman Characteristic Group Frequencies*, 3rd ed.; John Wiley & Sons: London UK, 2001; pp 219–220.



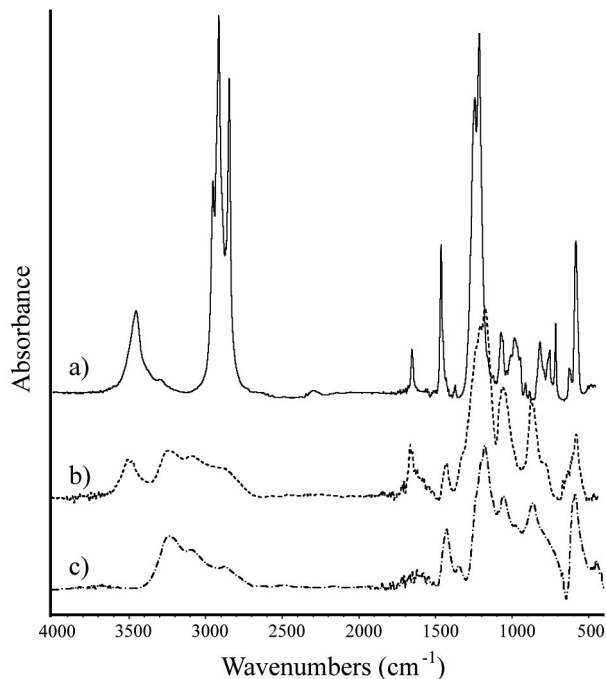


**Figure 2.** FTIR spectra of SDS: unaged (a); thermally aged at 120 °C for 48 h (b) and 500 h (c).

stretching band between 3000 and 3400  $\text{cm}^{-1}$ , a peak at 1418  $\text{cm}^{-1}$  tentatively assigned to bending vibrations of hydroxyl groups, and the shifting of the sulfate stretching toward lower wavenumbers (1200–1100  $\text{cm}^{-1}$ ). These are all evidence of the progressive SDS decomposition into alcohols and free sulfate ions.<sup>22</sup> SDS thermal oxidation also results in the release of volatile molecules, representing a significant fraction of the total weight loss of  $\sim 20\%$  after 500 h of aging.

This confirms that SDS, once exuded from the acrylic latex film, partially degrades into free sulfates, alcohols, and volatiles. Even if there is no evidence of other oxidation products, it is reasonable to assume that additional carbonyl derivatives had formed as intermediate compounds or volatiles during the degradation process.<sup>23</sup>

Triton X-405, a nonylphenol polyethoxylated nonionic surfactant, was not detected on the film surface since its weight percentage in the latex formulation was very low, and it undergoes fast photooxidative and thermal degradation. In fact, polyethoxylated surfactants degrade much faster than alkyl sulfates. For example, Triton X-405 lost 57.4% of its weight after 500 h of thermal aging at 120 °C, and it volatilized almost completely under an extended accelerated light aging.

The infrared spectra of the nonionic surfactant, recorded at given intervals to monitor the effects of thermal or light aging, were completely different from those of the unaged surfactant already after the first 24 h of treatment. The decrease in the intensity of absorption throughout the whole spectral range indicates that degradation proceeds via scission reactions and loss of volatile fragments. Bond cleavages occurs in both the ethoxylated and alkyl chain, as demon-

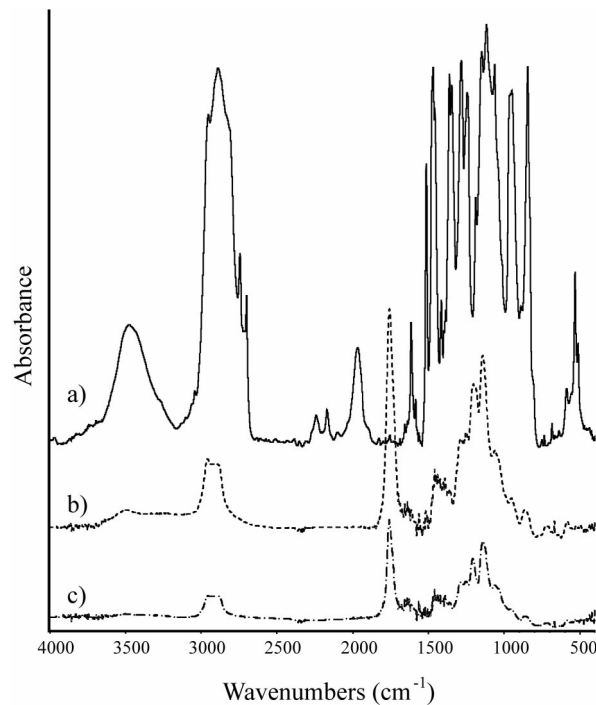


**Figure 3.** FTIR spectra of Triton X-405: unaged (a); thermal aging at 120 °C for 48 h (b) and 500 h (c).

strated by the strong decrease of methylene and ether vibration modes between 1460 and 840  $\text{cm}^{-1}$ , as well as in the aromatic moiety, as demonstrated by the disappearance of the aromatic ring absorptions at 1610, 1580, and 1512  $\text{cm}^{-1}$  (Figure 3).

Similarly to the case of high molecular weight poly(ethylene oxide), oxidation of the polyethoxylated surfactant proceeds through a radical mechanism via oxygen attack on carbon atoms in  $\alpha$ -positions which leads to ethylene oxide chain cleavage and the formation of ester groups and formates.<sup>24</sup> At the initial stage of the process, ester (1750 and 1140  $\text{cm}^{-1}$ ) and formate groups (1725 and 1190  $\text{cm}^{-1}$ ) develop approximately at the same rate, but with the progression of the aging ester formation prevails. Low molecular weight degradation products such as acidic compounds, ethylene glycols, and  $\text{CO}_2$  are released as volatiles.<sup>25</sup>

**Mapping of Surfactant Surface Distribution by  $\mu\text{ATR-FTIR}$ .** The surfactant distribution at the surface of the waterborne acrylic coatings was also studied by  $\mu\text{ATR-FTIR}$  mapping. Areas of  $700 \times 700 \mu\text{m}$  were analyzed. Color maps obtained by calculating the height ratio of two peaks, one characteristic of the acrylic medium (1238  $\text{cm}^{-1}$ ) and the other diagnostic of surfactants (1108  $\text{cm}^{-1}$ ), are reported in Figure 4. While the map of the as-cast dried sample (a) was chromatically homogeneous, the one obtained after heating the film at 120 °C for 2 h (b) showed an increased intensity of the infrared absorption due to the surfactant, which is indicated by the greenish-blueish areas. Surfactants cover almost all of the film surface; however, their distribution

(22) Lea, J.; Adesina, A. A. *J. Photochem. Photobiol. A: Chem.* **1998**, *118*, 111.

(23) Hidaka, H.; Zhao, J.; Pelizzetti, E.; Serpone, N. *J. Phys. Chem.* **1992**, *96*, 2226.

(24) Morlat, S.; Gardette, J.-L. *Polymer* **2001**, *42*, 6071.

(25) Pelizzetti, E.; Minero, C.; Maurino, V.; Sciafani, A.; Hidaka, H.; Serpone, N. *Environ. Sci. Technol.* **1989**, *23*, 1380.

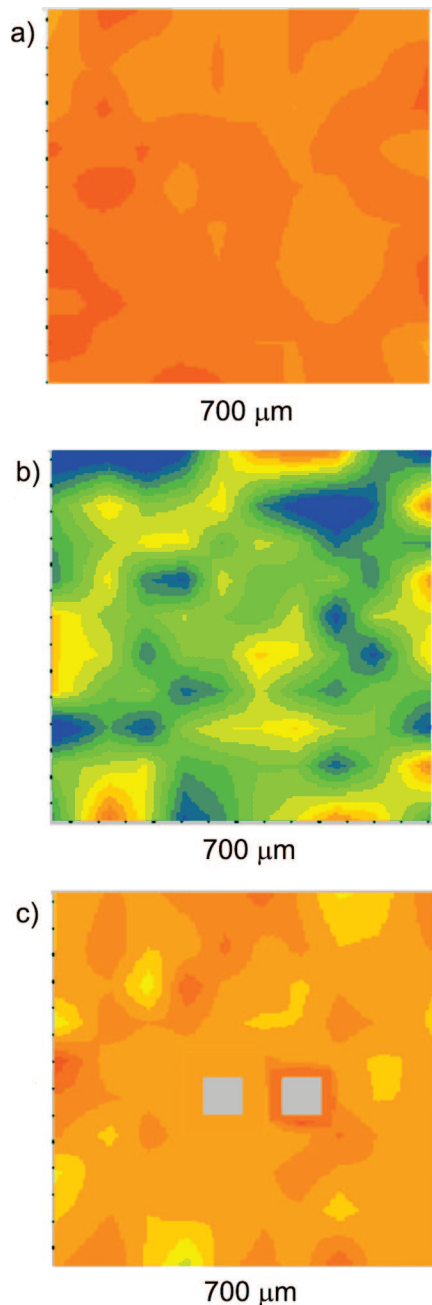


**Figure 4.**  $\mu$ ATR-FTIR maps of the acrylic latex film aged at room temperature for a few days (a), after thermal aging at 120 °C for 2 h (b), and after thermal aging and rinsing with water (c).

appears fairly inhomogeneous with areas of a high surfactant concentration (blue color) and others of low concentration where surfactants were hardly (yellow) or absolutely not detected (orange). After rinsing with distilled water the surfactants were efficiently removed from the coating surface (c), and the resulting map had the same colors and color distribution of the original coating.

**Surface Morphological Characterization by Atomic Force Microscopy.** In order to investigate the surface morphology in a better spatially resolved detail, the surface morphology of the acrylic films was analyzed by atomic force microscopy. On the surface of the latexes film dried at room temperature discrete polymer particles could be easily identified (Figure 5a). The polymer particles were observed to retain their individual identity for several days even if

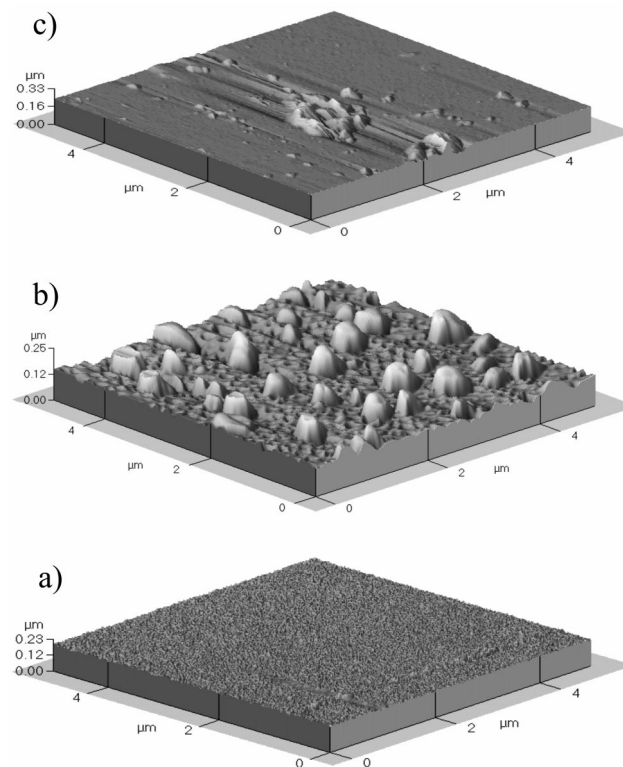


**Figure 5.** 3D AFM topographic images ( $5 \times 5 \mu\text{m}$ ) of the acrylic latex film as-cast at room temperature (a) and after annealing at 120 °C for 170 h (b) and 500 h (c).

the low  $T_g$  of the p(nBA-co-MMA) copolymer had allowed effective particle deformation with establishment of intimate and continuous interparticle contact. This film appeared optically transparent and possessed mechanical integrity, indicating completeness of film formation, even though coalescence had only occurred up to a limited extent.

The occurrence of a net migration of surfactant molecules in a given direction largely depends on the interactions of the surfactants among themselves, with the polymer, and with the support of the polymer film. In the cases of polymer coatings applied as thin films on glass slides, surfactants were observed to preferentially exude at the polymer/air interface.

After heating at 120 °C for 2 h complete coalescence had occurred, and at the same time surfactant molecules appeared to be rapidly exuded from the film, forming bulges and leaving craters on the surface (Figure 5b). The amount of exuded material increased over time and bulges, much larger in size than the original individual polymer particles, built up at the polymer/air interface. However, after 500 h of thermal aging the amount of surfactant had considerably decreased as a result of partial degradation and volatilization (Figure 5c). The film surface was mainly characterized by cavities surrounded by residues of surfactants and possibly other low molecular weight degradation byproduct.

The above AFM results indicate that surfactants contained in a waterborne coating undergo thermooxidative degradation more slowly than expected from the kinetics of degradation determined by infrared spectroscopy and gravimetric measurements on pure surfactants. When embedded in a polymer matrix, the thermooxidative stability of surfactants clearly depends on the oxygen concentration and availability, and

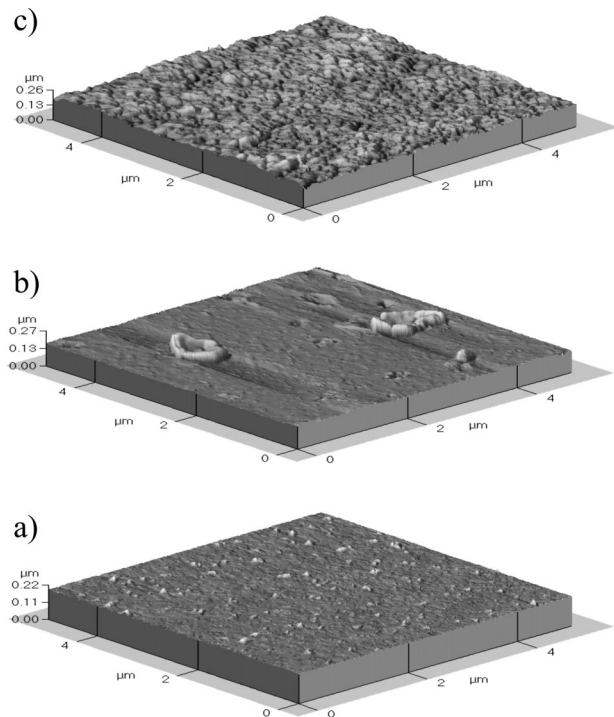


**Figure 6.** 3D AFM topographic images ( $5 \times 5 \mu\text{m}$ ) of the acrylic latex film artificially light aged under a xenon lamp after 500 h (a), after 1000 h (b), and after rinsing with water (c).

the rate of degradation is related to their diffusion rates toward the film surface. Under thermal aging at temperatures much higher than the polymer glass transition, diffusion of low molecular weight additives, such as surfactants, is promoted and results in phase separation of hydrophilic domains.

Aging experiments under solar light irradiation were performed at room temperature, that is, slightly below the glass transition temperature and thus with a reduced mobility of surfactants. Figure 6 shows the AFM images of the light aged acrylic film. Once exuded the surfactants are homogeneously distributed on the polymer film surface (Figure 6a) and only at extended irradiation time (Figure 6b) do they self-assemble, building aggregates whose dimensions are comparable to those observed in the thermally aged samples. In Figure 6 the upper AFM image shows the effect of rinsing the surface with distilled water. As expected, surface bulges, being water soluble, had disappeared, and the surface below appeared rougher than the original one.

The development of the surface morphology can be seen in the section analysis of Figure 7 which shows the height profiles before and after different kinds of treatments. Soon after drying, the surface was characterized by a close-packed array of polymer particles (Figure 7a). The average particle diameter, calculated as the mean valley-to-valley distance in the plane, was 60 nm and was in accordance with the value obtained by light scattering measurements. The mean peak-to-valley distance in the vertical direction was  $\sim 15$  nm. After 500 h of artificial solar light irradiation (Figure 7b) the peak-to-valley distance in the plane increased, and complete coalescence occurred, causing the merging of the polymer particles. In the vertical direction, the maximum

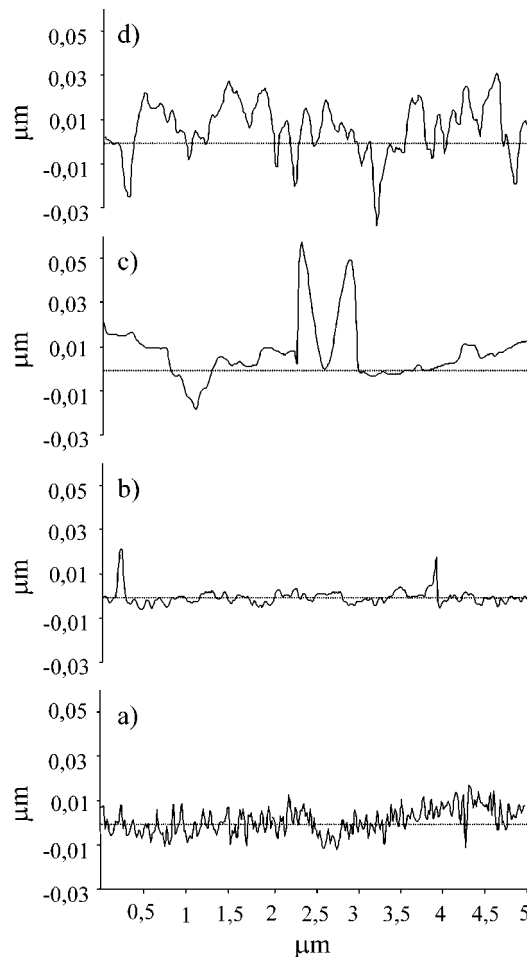


**Figure 7.** Section analysis of the latex film as-cast at room temperature (a), artificially light aged for 500 (b) and 1000 h (c), and artificially light aged for 1000 h and rinsed with water (d).

height had tripled because of the presence of protrusions on the polymer surface. By extending the aging treatment (Figure 7c), surface bulges increased in both height and width, while the other areas of the surface looked smoother. After rinsing with water (Figure 7d), the surface morphology was completely changed: all the aggregates were removed as well as the thin homogeneous layer of surfactants that covered the coating surface, revealing a rougher surface underneath. This behavior is relevant because it is well-known that roughness influences gloss and thus the appearance of the polymer coating, and it can also affect the interactions of the substrates with other solids and liquid substances.

## Conclusion

Both anionic and nonionic polyethoxylated surfactants are frequently used in the synthesis of polymer latexes as preferential nucleation sites of the radical reaction polymerization process and as stabilizing agents of the final colloidal dispersion. After water evaporation surfactants are trapped in the solid film, but being incompatible with the polymer, they diffuse forming hydrophilic domains and in the end migrate and protrude from the surface.

The chemical stability of the acrylic copolymer itself did not seem to be affected by the presence of surfactants and

of their degradation products. Under thermal aging the acrylic copolymer was stable, even if both the ionic and the nonionic surfactant degraded relatively fast. Also, under accelerated light aging the oxidation degree of the acrylic component was not very different from what is observed in coatings obtained from polymer solutions of similar compositions.<sup>19,20</sup> In any case, it cannot be excluded that upon extended aging the hydrophilic and oxidized small molecules, resulting from surfactant degradation, can sensitize the film surface to radical and photochemical degradation processes.

On the other hand, the results obtained in this study indicate indeed that the most relevant morphological and chemical changes that occur over time to waterborne acrylic coatings are primarily related to the exudation of surfactants.

Thermal treatments at temperatures much higher than the polymer glass transition promoted the diffusion of low molecular weight molecules, and in a few hours bulges of surfactants appeared on the film surface. Upon thermal aging both the anionic SDS and the nonionic Triton X-405 underwent fast thermal degradation, and at extended aging the amount of surfactant on the polymer surface significantly decreased.

Under light aging at room temperature the mobility of the surfactants was considerably lower than during thermal aging, and their exudation proceeded more slowly. In contrast to

the photolabile polyethoxylated surfactants, SDS is stable to solar light irradiation, and as a consequence its distribution on the film surface was not affected by photodegradation and essentially depended on diffusion factors.

Surface segregation of surfactants results in the formation of a highly hydrophilic layer at the air interface, and this will increase the coating wettability to different extents depending on the aging conditions.

At the same time, surfactant migration and local aggregation modify the overall film composition, producing chemical and physical heterogeneities that can generate stresses and failure of adhesion.

In a following paper, now in preparation, the effects of the presence of self-cross-linking groups modifying the acrylic polymer matrix will be presented, and their role in preventing surfactants from phase-segregating and from exuding to the coating surface will be discussed.

**Acknowledgment.** This work was realized with financial support by the Italian Ministry of University and Research, through the project "New polymers and innovative methodologies for consolidation and protection of stone materials", and partial support from the MIUR-NANOPACK FIRB 2003 program (project D.D.2186 Prot.N.RBNE03R78E).

CM0714077